

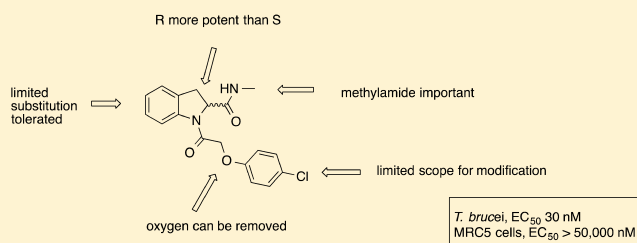
Discovery of Indoline-2-carboxamide Derivatives as a New Class of Brain-Penetrant Inhibitors of *Trypanosoma brucei*

Laura A. T. Cleghorn, Sébastien Albrecht, Laste Stojanovski, Frederick R. J. Simeons, Suzanne Norval, Robert Kime, Iain T. Collie, Manu De Rycker, Lorna Campbell, Irene Hallyburton, Julie A. Frearson, Paul G. Wyatt, Kevin D. Read, and Ian H. Gilbert*

Drug Discovery Unit, Division of Biological Chemistry and Drug Discovery, College of Life Sciences, University of Dundee, Sir James Black Centre, Dundee, DD1 5EH, U.K.

S Supporting Information

ABSTRACT: There is an urgent need for new, brain penetrant small molecules that target the central nervous system second stage of human African trypanosomiasis (HAT). We report that a series of novel indoline-2-carboxamides have been identified as inhibitors of *Trypanosoma brucei* from screening of a focused protease library against *Trypanosoma brucei brucei* in culture. We describe the optimization and characterization of this series. Potent antiproliferative activity was observed. The series demonstrated excellent pharmacokinetic properties, full cures in a stage 1 mouse model of HAT, and a partial cure in a stage 2 mouse model of HAT. Lack of tolerability prevented delivery of a fully curative regimen in the stage 2 mouse model and thus further progress of this series.



INTRODUCTION

Human African trypanosomiasis (HAT) or sleeping sickness occurs in sub-Saharan Africa and is caused by two subspecies of the protozoan parasite *Trypanosoma brucei*; *Trypanosoma brucei gambiense* in West and Central Africa and *Trypanosoma brucei rhodesiense* in East Africa. This neglected disease is transmitted by the bite of a tsetse fly and can be fatal if not treated. In 2009, the number of reported cases dropped to 10000 for the first time in 50 years; the trend continued in 2010 with around 7000 cases reported, although the estimated number of actual cases is 30000.^{1–3}

Many people in the affected populations live in remote areas with limited access to adequate health care, impeding diagnosis and treatment. There are two stages of the disease; in stage 1, the trypanosomes multiply in subcutaneous tissues, blood, and the lymphatic system, resulting in bouts of fever, headaches, joint pains, and itching. In the second stage, the parasites cross the blood–brain barrier to infect the central nervous system, leading to confusion, sensory disturbance, poor coordination and disruption of the sleep cycle, coma, and death. Unfortunately, diagnosis often does not occur until the patient has stage 2 disease. There is no effective vaccine.⁴ Pentamidine (*T. b. gambiense*) and suramin (*T. b. rhodesiense*) are currently used to treat infection at stage 1, while there are three treatments for stage 2: (i) melarsoprol, an arsenical, can be used to treat both strains but has severe side effects⁵ and is given by intravenous injection over an extended time period; (ii) eflornithine is less toxic than melarsoprol but only effective against *T. b. gambiense* strain and is not suitable for a rural African setting given the requirement for an extended period of intravenous dosage;^{6,7} and

(iii) in 2009, a combination treatment of nifurtimox and eflornithine (NECT) was introduced, although this is also not effective against *T. b. rhodesiense*.^{8–10}

There is undeniably a need to identify new, safer, and easier to use antitrypanosomal agents that can cross the blood–brain barrier to be suitable for use as a stage 2 therapy. The ideal candidate would be one that is suitable for treating both the stage 1 (peripheral) and stage 2 (CNS) infection.¹¹

One strategy used in the Drug Discovery Unit in Dundee to find new starting points is phenotypic (in vitro whole cell) screening of compounds against *Trypanosoma brucei brucei*. A mammalian cell counter screen, for example MRC-5 cells, is then used as a counter screen to exclude nonselective compounds.^{12–14} Using this approach, our in-house designed protease set (~3400 compounds) was screened against *T. b. brucei*. The protease library was selected by analysis of known protease inhibitors from the literature to identify motifs that are found to bind to proteases. A selection of compounds was then made that contained these motifs and retained lead-like properties (generally compliant with the rule of 4).¹⁵ From the primary screening, carried out at single concentration, 93 compounds showed a greater than 50% inhibition of parasite growth at 30 μ M. The hits from the single-point screen were cherry-picked and rescreened to determine potency (EC_{50} value). This led to identification of a series of indoline-2-carboxamides, typified by **1** (Figure 1).

Received: April 17, 2015

Published: September 29, 2015

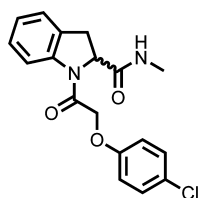


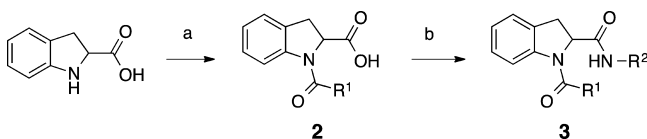
Figure 1. Hit (1) identified from the screen.

Compound 1 was the most potent example in the series of indoline-2-carboxamides identified from screening, showing good antiproliferative activity ($EC_{50} = 27$ nM) with selectivity over mammalian cells (>1600 -fold). As a starting point, compound 1 contained several desirable features for a potential therapeutic agent for stage 2 HAT: low molecular weight (344), clogP (2.4) compatible with oral and CNS bioavailability, and low PSA (59 Å²). These properties are all consistent with CNS penetration, and 1 was predicted to cross the blood–brain barrier using StarDrop (www.optibrium.com). Early in vitro DMPK profiling indicated a good plasma protein free fraction (fraction unbound, mouse (F_u) = 0.26) and solubility (>100 μg mL⁻¹), although the hepatic microsomal turnover was higher than desired. The measured intrinsic clearance (Cl_{int}) for the compound was mouse/rat/human = 4.4/4.4/2.6 mL min⁻¹ g⁻¹. Phenoxyacyl diamide indolines have not previously been described in the literature as potential drug candidates in other disease areas. A chemistry program was initiated to optimize the original hit. To satisfy the target product profile for stage 2 HAT, the molecule should be blood–brain barrier penetrant. Ideally, the compound should also be orally bioavailable. Therefore, the initial aim was to increase potency and improve metabolic stability while retaining a low PSA (ideally <70 Å²),¹⁶ low MW, low clogP, and a high fraction unbound.^{17–19}

CHEMISTRY

Two routes were employed to synthesize the indoline-2-carboxamides with an unsubstituted aromatic core. In the first route, 2-indolinecarboxylic acid (enantiomerically pure *R* and *S* are available commercially) was reacted in a two-step one-pot synthesis (Scheme 1). First, it was coupled to an appropriate

Scheme 1^a



^aConditions: (a) R^1CO_2H (1 equiv), TBTU, (1 equiv), DIPEA, DCM, room temperature, 2 h or R^1COCl (1 equiv), TEA, DCM, 0 °C to room temperature, 2 h; (b) R^2NH_2 (2 equiv), TBTU, (1 equiv), DIPEA, room temperature, 2 h, 2–85% yield for steps (a) and (b) combined. R^1 and R^2 are the substituents, as exemplified in Tables 1 and 3–6.

carboxylic acid using *O*-(benzotriazol-1-yl)-*N,N,N',N'*-tetramethyluronium tetrafluoroborate (TBTU) as the peptide coupling agent, and second to an appropriate amine, again in the presence of TBTU. Alternatively, R^1 could be introduced using an acid chloride.

There are only a limited number of substituted 2-indolinecarboxylic acids available commercially. Several routes were developed to achieve different substitution patterns on the

aromatic ring (Scheme 2). In the most general procedure, a range of substituted indolines was prepared starting with methyl azidoacetate 4, which was formed from sodium azide and methyl bromoacetate. Upon reaction with an aldehyde, this formed vinylazide 5.²⁰ A rhodium-catalyzed reaction was utilized to cyclize vinylazide 5 to indole 6.²¹ Reduction using magnesium turnings afforded the desired methyl indolinecarboxylate 7²² that was subsequently reacted with methylamine and then the appropriate acid chloride to yield aromatically substituted diamide indolines 8. In the case of 5-fluoroindoline, higher yields were achieved using an alternative synthesis (9–13).^{23–25} 5-Fluoro-2-iodobenzoic acid was reduced with borane, and the resulting alcohol reacted to form mesylate 9, which was reacted with *N*-(diphenylmethylene)glycine ethyl ester to give ethyl 2-((diphenylmethylene)amino)-3-(5-fluoro-2-iodophenyl)propanoate 10. The amine was deprotected with citric acid and reacted with the desired acid in a standard TBTU coupling to give 11. The indoline ring was cyclized by copper catalysis and the ethyl ester hydrolyzed with lithium hydroxide to give 12. Reaction with methylamine and TBTU afforded the desired 5-fluoroindoline diamide 13.

An enantiomerically pure synthesis of the substituted indoline core was also carried out using a literature procedure (Scheme 3).²⁶ A racemic mixture of methyl indolinecarboxylate 7 was reacted with commercially available lipase A, *Candida antarctica* CAL-A (CLEA) and allyl 3-methoxyphenyl carbonate (14) to afford a 50:50 mixture of the (*R*)-methylindoline-2-carboxylate 15 and (*S*)-1-allyl-2-methylindoline-1,2-dicarboxylate 16, which were separable by column chromatography. Details of other synthetic routes used to synthesize individual compounds are described in the Supporting Information.

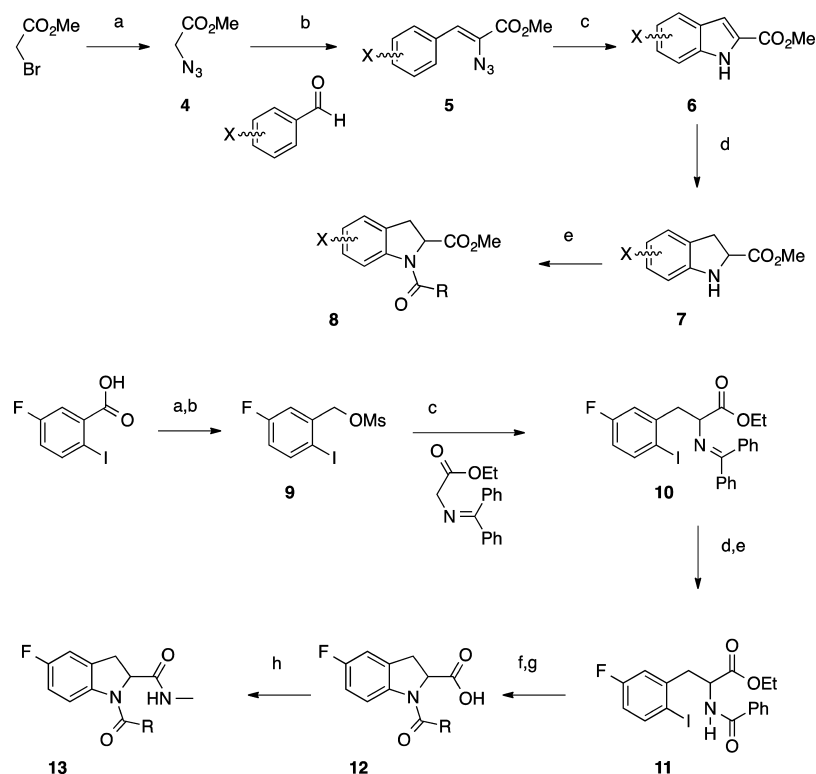
RESULTS AND DISCUSSION

All compounds were screened using a *T. b. brucei* whole cell parasite assay²⁷ and counter screened against a mammalian MRC-5 cell line to exclude any compounds that showed general cytotoxicity. None of the compounds reported here showed any toxicity in the counter screen.

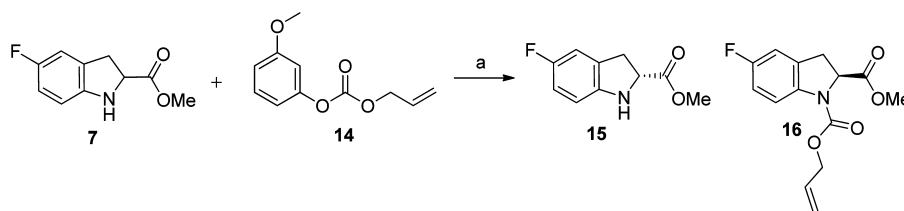
Initial Hits. An initial hit expansion was carried out with 10 indoline-2-carboxamides contained within our protease set and a further small number of analogues that were commercially available. Table 1 illustrates selected results. The potency data from the screening hits and commercially available hit expansion compounds showed the general trend that NHMe $>$ NHEt $>$ NH₂ at the R^2 position. Both ether and benzyl pendants at R^1 showed potential for further development. Early investigations established that there were defined structure–activity relationships, indicating a precise molecular target(s). Thus, changing the R^2 amine and varying R^1 could dramatically change the potency.

Enantiomers. Examination of the individual enantiomers of 1 showed that (*R*)-isomer (27) was ~1400-fold more potent (EC_{50} value) than (*S*)-isomer (26), although the single enantiomers displayed a similar level of hepatic microsomal turnover to the racemic 1 (Table 2). Initial work focused on using the racemic 2-indolinecarboxylic acid, as it was found to be equipotent within experimental error to the (*R*)-enantiomer; subsequently, analogues of interest were synthesized as the (*R*)-enantiomer.

Initial Evaluation. To follow up the initial screening, we initiated a more extensive hit-to-lead evaluation. There were essentially three points on the indoline-2-carboxamide scaffold that could be explored to look for improvements in potency

Scheme 2^a

^aConditions (4–8): (a) NaN₃, DMF, 0 °C to room temperature, 16 h, under Ar; (b) methyl azidoacetate (3 mol equiv), aldehyde (1 mol equiv), THF, NaOMe, MeOH, –10 °C, 3 h; (c) Rh₂(O₂CCF₃)₄, toluene, 65 °C, 48 h; (d) Mg, MeOH, 0 °C to room temperature, 16 h, under Ar; (e) MeNH₂ in THF, room temperature, 16 h, then RCOCl, DIPEA, DCM, room temperature under argon. Conditions (9–13): (a) BH₃, 1 M in THF 0 °C to room temperature, 16 h; (b) MsCl, DIPEA, THF, 0 °C, 2 h; (c) TBAI, 5 mol % in toluene, 50% (w/v) NaOH, 0 °C to room temperature, 16 h; (d) citric acid, 0 °C to room temperature, 3 h; (e) RCO₂H, TBTU, DIPEA, room temperature, 2 h; (f) CsOAc, CuI, DMSO, room temperature, 1.5 h; (g) LiOH, THF, room temperature; (h) TBTU, MeNH₂ (2 M in MeOH), DCM, room temperature, 2 h. Overall 46% yield from commercially available 5-fluoro-2-iodobenzoic acid.

Scheme 3^a

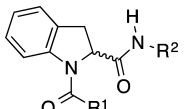
^aConditions: (a) lipase Cal-A, TBME, room temperature, 5 h, under argon, 35% of 15 (expect 50%, 70% of desired product overall).

(Figure 2) and ideally to reduce the hepatic microsomal turnover. First, looking at the R¹ pendant substituent both as two-carbon ether and one-carbon linkers (A); second, varying the R² amine (B); and last, investigating alternative cores such as aza indoline, tetrahydroquinoline, and substituted indolines (C). Analysis of compound 1 using a cytochrome P450 (P450) metabolism predictor (StarDrop) suggested that metabolism of the 5-position of the indoline may be contributing to metabolic instability.

Variation of the Pendant Ether. Initially, the substituent on the ether was varied to block potentially metabolically labile positions and attempt to improve potency by finding new interactions (Table 3). The activity was generally found to be very sensitive to the nature of the substituent. Increasing chain length and flexibility by incorporating a benzyl ether 28 led to ~70-fold loss in potency (as measured by EC₅₀ value). The 3-

fluorophenyl derivative 29 was found to be equipotent to 1 but showed no improvement in intrinsic clearance. A chloro in the 3-position of 30 led to a 15-fold loss in potency and a significant increase in intrinsic clearance. An unsubstituted phenyl 31 was found to be equipotent, indicating that halogens are not necessarily required for binding in the active site. Interestingly, this compound showed an increased intrinsic clearance for mouse and rat but a similar level for human. Replacing the aromatic group with an aliphatic such as 3-tetrahydropyran 32 showed a 37-fold loss in potency; however, a much lower intrinsic clearance was observed. A heteroaromatic ring (pyridine) 33 was tolerated, although a 10-fold loss in potency was observed. 4-Methyl 34 and 4-fluoro 35 are equipotent with 1 within experimental error. The 4-fluoro showed improved intrinsic clearance (at least in mice). The single (R)-enantiomer of this was synthesized 36 and had a similar profile. 3,4-

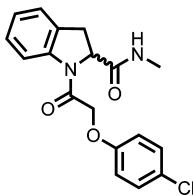
Table 1. Potency of Selected Initial Screening Hits and Commercially Available Hit Expansion



Compound	R ¹	R ²	<i>T. b. brucei</i> EC ₅₀ (μM) ^a	MRC-5 EC ₅₀ (μM) ^a
1		Me	0.03	> 50
17		Me	0.31	> 50
18		Me	2.9	> 50
19		Me	0.45	> 50
20		Me	0.66	> 50
21		Me	0.22	> 15 ^b
22		Et	0.65	> 50
23		Et	0.99	> 50
24		H	13	> 50
25		H	> 50	> 50

^aEC₅₀ values are shown as mean values of two or more determinations. Standard deviation is typically within 2–3-fold from the EC₅₀. ^bThe upper concentration was set to 15 μM not 50 μM in this assay.

Table 2. Stereochemical Investigation around the Original Hit



	<i>T. b. brucei</i> EC ₅₀ (μM) ^a	MRC-5 EC ₅₀ (μM) ^a	mouse microsomal intrinsic clearance (mL min ⁻¹ g ⁻¹)
1	0.027	>50	4.4
(S)-26	41	>50	4.0
(R)-27	0.029	>50	3.6

^aEC₅₀ values are shown as mean values of two or more determinations. Standard deviation is typically within 2–3-fold from the EC₅₀.

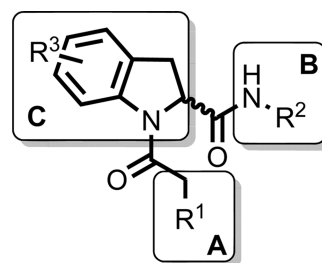


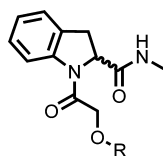
Figure 2. Planned optimization studies of the hit compound.

Difluorophenyl **37** was synthesized as a single enantiomer and was equipotent to **1**.

Variation of the Benzyl Moiety. The pendant ether was replaced by a methylene linker to give a series of benzyl derivatives. Switching to a benzyl slightly lowered the PSA; such modifications are favorable when designing a molecule to cross the BBB. The SAR observed for the benzyl derivatives (Table 4) followed a similar trend to that observed in the pendant ether series. For comparison purposes, **21**, an unelaborated phenyl with a potency of 0.22 μM, was used as the start point in this study. Increasing the steric bulk of the pendant substituent from phenyl to naphthyl **39** showed complete loss of potency, suggesting there is a limited space in the adopted binding pose. The 4-chlorophenyl analogue **40** showed approximately 3-fold improvement in activity; however, it had the same intrinsic clearance as **1**. Bulky alkyl group substituents on the aromatic ring such as isopropyl **41** were not well tolerated and led to a significant increase in mouse intrinsic clearance (35 mL min⁻¹ g⁻¹). 4-Trifluorophenyl **42** and 4-fluorophenyl **43** were equipotent at 0.1 μM. Compound **43** showed very good metabolic stability, similar to that observed for 4-fluorophenyl **35** in the ether series. Addition of a fluoro in the 2-position was detrimental to activity when combined with 4-fluoro **44**. A fluoro in the 3-position either with 4-chloro **45** or 4-fluoro **46** did not significantly affect the potency and displayed a detrimental effect on metabolic stability, particularly in the case of the 4-chloro derivative. The (*R*)-enantiomer of **43**, **47**, retained good potency, showed improved metabolic stability, lower plasma protein binding compared to the “best” original hit **1** (*F*_w, mouse [fraction unbound] 0.59 vs 0.26) combined with a good free fraction in brain tissue (*F*_w, male SD rat = 0.43).

Methylamide Replacements. The methylamide substituent was investigated to see if potency improvements could be gained at this position and because the methyl group is a point of potential metabolic vulnerability (Table 5). Investigation into the methylamine suggested that there were space limitations around this section of the molecule in the binding pocket. Capping the free NH of **48** gave a 200-fold drop in potency, suggesting either the NH is important for binding or substituents in two different vectors were not tolerated because of steric restrictions. Extending the chain length from methyl to ethyl **49** showed a slight loss in potency yet extending to butyl amine **50** was not tolerated, leading to ~700 fold loss in potency together with a dramatically increased metabolic instability. Incorporating a slightly bulkier group such as a cyclopropyl **51** resulted in ~14-fold drop in potency, again hinting at size limitations within the pocket as observed with **48**. Fluorination of the ethylamine substituent at the methyl group **52** gave ~17-fold loss in potency compared to the ethylamine substituent. In an attempt to improve the metabolic stability a methylamine-*d*₃ analogue was synthesized **53**; deuteration has previously been reported as a

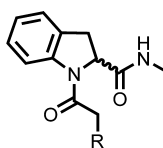
Table 3. Pendant Ether Modifications



compd no.	stereochem	R	<i>T. b. brucei</i> EC ₅₀ (μM) ^a	MRC-5 EC ₅₀ (μM) ^a	microsomal intrinsic clearance ^b (mL min ⁻¹ g ⁻¹)		
					m	r	h
1	R/S	4-chlorophenyl	0.03	>50	4.4	4.4	2.6
28	R/S	benzyl	1.9	>50	ND	ND	ND
29	R/S	4-chloro-3-fluorophenyl	0.03	>50	4.4	13.5	3.3
30	R/S	3,4-dichlorophenyl	0.40	>50	9.1	ND	ND
31	R/S	phenyl	0.04	>50	6.9	9.0	1.4
32	R/S	3-tetrahydropyran	1.1	>50	1.2	ND	ND
33	R	4-methyl-3-pyridyl	0.39	>50	ND	ND	ND
34	R/S	4-methylphenyl	0.03	>50	6.5	47	2.4
35	R/S	4-fluorophenyl	0.02	>50	1.2	ND	ND
36	R	4-fluorophenyl	0.04	>50	1.2	4.9	1.3
37	R	3,4-difluorophenyl	0.03	>50	3.2	ND	ND
38	R	phenyl-d ⁵	0.05	>50	ND	ND	ND

^aEC₅₀ values are shown as mean values of two or more determinations. Standard deviation is typically within 2–3-fold from the EC₅₀. ^bm/r/h = mouse/rat/human; ND = not determined.

Table 4. Benzyl Analogues



compd no.	stereochem	R	<i>T. b. brucei</i> EC ₅₀ (μM) ^a	MRC-5 EC ₅₀ (μM) ^a	mouse microsomal intrinsic clearance (mL min ⁻¹ g ⁻¹)
21	R/S	phenyl	0.22	>15	ND
39	R/S	1-naphthyl	50	>50	28
40	R/S	4-chlorophenyl	0.08	>50	4.4
41	R/S	4-isopropylphenyl	0.77	>50	35
42	R/S	4-trifluoromethylphenyl	0.11	>50	3.0
43	R/S	4-fluorophenyl	0.11	>50	0.8
44	R/S	2,4-difluorophenyl	2.3	>50	0.5
45	R	4-chloro-3-fluorophenyl	0.08	>50	8.4
46	R/S	3,4-difluorophenyl	0.11	>50	1.9
47	R	4-fluorophenyl	0.05	>50	1.9

^aEC₅₀ values are shown as mean values of two or more determinations. Standard deviation is typically within 2–3-fold from the EC₅₀. ND = not determined.

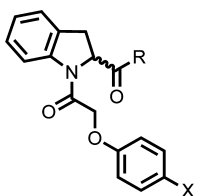
method to reduce metabolism.²⁸ Deuterated compound **53** was equipotent with improved metabolic stability compared to **1** and was similar to the undeuterated analogue **35**.

Core Modifications. Examination of **1** in a P450 metabolism predictor (StarDrop) suggested that metabolism of the 5-position of the indoline may be responsible for the observed metabolic instability. In an attempt to block this potential metabolic hot spot, synthesis was undertaken to replace the hydrogen in this position with a fluorine, a strategy frequently employed in medicinal chemistry that would hopefully not impair binding or reduce the observed antiproliferative effect.²⁹ Substituted indolines were prepared using the procedure described in the Chemistry section (Scheme 2; compounds made are listed in Table 6). 5-Fluoro indoline **54** was well tolerated with a marginal loss in potency compared to **1** but only marginal improvement in metabolic stability observed, if any. 5-Fluoroindoline with a 4-fluorophenyl as the pendant ether

moiety **55** showed improved metabolic stability with a good plasma protein free fraction ($F_u = 0.33$ mouse). The potency and metabolic stability were similar to the nonfluorinated indoline **43**. Compound **55** also showed a good free fraction in brain tissue ($F_u = 0.29$ rat). The (*R*)-isomer equivalent of **55**, **56**, was also well tolerated. The addition of a fluoro substituent to the 6-position **57**, 7-position **58**, or 4 and 6-positions **59** on the aromatic portion of the indoline gave equipotent results but offered no advantage over earlier compounds. The 5-bromoindoline analogue **60** was found to be equipotent, suggesting there may be a large amount of space surrounding the aromatic portion of the indoline in the binding mode. To test this further, the 5-phenyl (**61**) and 5-(4-pyridyl) (**62**) derivatives were synthesized; both led to approximately a 10-fold loss in potency, and substituents in the position were not pursued further.

Alternative cores to the indoline were also examined: replacing the indoline with pyrrolidine **64**, removing the C3 carbon of the

Table 5. Amide Modifications

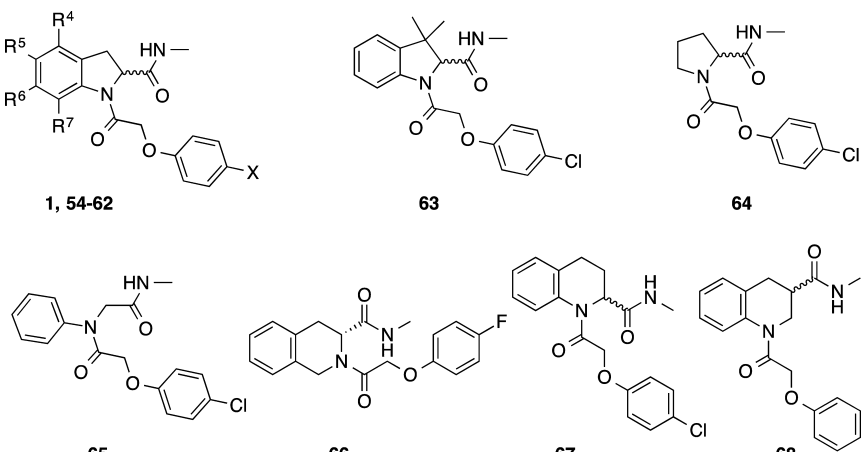


X = F, Cl

compd no.	stereochem	X	R	<i>T. b. brucei</i> EC ₅₀ (μM) ^a	MRC-5 EC ₅₀ (μM) ^a	mouse microsomal intrinsic clearance (mL min ⁻¹ g ⁻¹)
1	R/S	Cl	MeNH–	0.03	>50	4.4
48	R/S	Cl	Me ₂ N–	5.4	>50	ND
49	R/S	Cl	EtNH–	0.09	>50	6.2
50	R/S	Cl	<i>n</i> -BuNH–	19	>50	27
51	R/S	Cl	cyclopropyl-NH–	0.41	>50	5.5
52	R/S	Cl	CF ₃ CH ₂ NH–	1.5	>50	9.0
53	R	F	<i>d</i> ³ -MeNH–	0.04	>50	1.9

^aEC₅₀ values are shown as mean values of two or more determinations. Standard deviation is typically within 2–3-fold from the EC₅₀. ND = not determined.

Table 6. Core Modifications



compd no.	stereochem	X	R ⁴	R ⁵	R ⁶	R ⁷	<i>T. b. brucei</i> EC ₅₀ (μM) ^a	MRC-5 EC ₅₀ (μM) ^a	microsomal intrinsic clearance (mL min ⁻¹ g ⁻¹) ^b		
									m	r	h
1	R/S	Cl	H	H	H	H	0.03	>50	4.4	4.4	2.6
54	R/S	Cl	H	F	H	H	0.06	>50	2.8	5.3	1.6
55	R/S	F	H	F	H	H	0.08	>50	1.3	2.1	0.5
56	R	F	H	F	H	H	0.04	>50	ND	ND	ND
57	R/S	F	H	F	F	H	0.09	>50	2.0	2.8	1.9
58	R/S	F	H	F	H	F	0.08	>50	2.9	ND	ND
59	R/S	Cl	F	F	F	H	0.07	>50	3.7	6.7	4.3
60	R/S	F	H	Br	H	H	0.08	>50	4.6	ND	ND
61	R/S	F	H	Ph	H	H	0.24	>50	ND	25	ND
62	R/S	F	H	4-pyridyl	H	H	0.44	>50	ND	ND	ND
63	R/S	Cl	NA ^c	NA	NA	NA	0.92	>50	14	ND	ND
64		Cl	NA	NA	NA	NA	36	>50	ND	ND	ND
65		Cl	NA	NA	NA	NA	19	>50	4.7	ND	ND
66	R	F	NA	NA	NA	NA	37	>50	ND	ND	ND
67	R/S	Cl	NA	NA	NA	NA	0.46	>50	ND	ND	ND
68	R/S		NA	NA	NA	NA	>50	>50	ND	ND	ND

^aEC₅₀ values are shown as mean values of two or more determinations. Standard deviation is typically within 2–3 fold from the EC₅₀. ^bm/r/h = mouse/rat/human. Synthetic scheme outlined in Supporting Information,³⁰. ND = not determined. ^cNA = not applicable.

indoline to give an open chain phenyl acetamide derivative **65**, or using 1,2,3,4-tetrahydroisoquinoline **66**. None were tolerated. However, the 1,2,3,4-tetrahydroquinoline derivative **67** was

moderately well tolerated with submicromolar potency. When the amide was moved to the 3-position (**68**), no activity was observed, indicating that the shape and proximity of the amide is

Table 7. In Vitro Data for Key Compounds

	1	27	35	47	55
<i>T. brucei</i> EC ₅₀ (μM) ^a	0.03	0.03	0.02	0.06	0.08
Hill slope	3.5	2.0		2.8	4.4
selectivity vs MRC-5	>1800	>1800	>2700	>860	>720
MWT	345	344	328	312	346
clogP	2.4	2.4	1.9	2.0	2.1
PSA	59	59	59	49	58
solubility	>100 μg/mL	ND	ND	64 μg/mL	>100 μg/mL
plasma protein binding	F _u = 0.26 (mouse)	F _u = 0.16 (rat)	F _u = 0.42 (mouse)	F _u = 0.59 (mouse)	F _u = 0.33 (mouse)
brain tissue binding (rat)	F _u = 0.15	ND	ND	F _u = 0.43	F _u = 0.29
microsomal intrinsic clearance (m/h) (mL min ⁻¹ g ⁻¹) ^b	4.4/2.6	3.6/ND	1.2/ND	1.9/ND	1.3/<0.5

^aEC₅₀ values are shown as mean values of two or more determinations. Standard deviation is typically within 2–3-fold from the EC₅₀. ^bm/h = mouse/human. ND = not determined. cLogP and PSA calculated using StarDrop. MWT = molecular weight; PSA = polar surface area; F_u = fraction unbound.

important in the active binding pose. In an attempt to further improve the metabolic stability, 3,3-dimethyl indoline **63** was synthesized; unfortunately, this gave ~34-fold loss in potency.

The molecular target (or targets) of these compounds is unknown. However, there is a very tight structure–activity relationship. It could be that the indoline-2-carboxamides may be working on more than one target, the overlapping needs for the SAR of each target resulting in a very tight SAR picture. Both the pendant ethers or benzyl groups give a very similar SAR, so it is possible with the flexibility of the linker chain that the substituents are free to rotate and occupy very similar space. There is a substantial difference between the enantiomers of the indoline-2-carboxamide, with the *R*-isomer being >1350-fold more potent than the *S*. The space around the methyl amide is very constrained as exceptionally few modifications are tolerated in this position, and removing the methyl to give an unsubstituted amide results in a loss of potency as does extending it. Substituted indolines are well tolerated, although no potency gains were observed. Substituting with large aromatic groups is tolerated in the 5-position, suggesting that there is a large space surrounding this part of the molecule that plays no role in the antiproliferative effect. Improved metabolic stability is observed with some of the substituted cores (e.g., 5-fluoroindoline). Alternative cores are moderately well tolerated but offer no improvement in physiochemical or antiproliferative properties.

■ DRUG METABOLISM AND PHARMACOKINETICS

Analysis of the measured in vitro DMPK data indicated that, in general, molecules synthesized with a higher predicted Log *P* (StarDrop) showed a higher metabolic instability when incubated with pooled mouse liver microsomes; compounds with intrinsic clearance in the desired range of <5 mL min⁻¹ g⁻¹ had a cLogP < 2. In general, the compounds showed a good plasma free fraction; with the nonether benzyl series having a slightly higher free fraction.

Five key molecules were selected for more detailed investigation. These were selected on the basis of potency, microsomal stability, and some diversity in structure. Thus, **1** is the start point, **27** the most active enantiomer, **35** is the fluoro analogue, **47** is where the ether oxygen has been removed, and **55** is where there is a fluorine in the indoline ring to increase the metabolic stability. A summary of the in vitro profile and mouse pharmacokinetic data are shown in Tables 7 and 8, respectively. The compounds selected all had drug-like properties: molecular weight around 350, clogP around 2, and PSA < 60 Å², which is

consistent with blood–brain barrier penetration and relatively low plasma protein binding.

Achieving Proof of Concept for the Series. Compound **1** had a higher than ideal microsomal metabolic instability in mouse (Cl_{int} 4.4 mL min⁻¹ g⁻¹) and when dosed intraperitoneally to female NMRI mice (*n* = 3) at 10 mg/kg, half-life was short (0.7 h), with blood free concentration below EC₅₀ within 2 h of dosing (Tables 7 and 8). Therefore, to try and achieve in vivo proof of concept for the series, the pharmacokinetics of **1** was assessed in HRN hepatic CYP reductase null mice³¹ (*n* = 3) following a single intraperitoneal (IP) dose at 10 mg/kg. With the absence of hepatic CYP450 activity, a significant improvement in exposure was observed (~9-fold higher AUC and half-life increasing to 4.8 h). Notably, blood free concentration remained significantly higher than EC₉₉ for 8 h, such that a b.i.d. dose regimen at greater than 2 mg/kg IP should deliver cures in a mouse model of infection, assuming linearity of exposure. From previous work (unpublished), *T. b. brucei* infection develops in female HRN mice consistently as for female NMRI mice, making it a useful model for rapid in vivo proof of concept for HAT with compounds poorly optimized for stability to CYP450s, thus allowing commitment to medicinal chemistry.

Compound **1** was therefore progressed to a stage 1 mouse model of HAT using HRN mice infected with *T. b. brucei* S427. Compound **1** was dosed (*n* = 3 infected mice) at 3 mg/kg IP b.i.d. for 4 d, starting 3 d post infection. Parasitaemia was knocked down and no relapse was observed up to 30 d post infection, confirming full cures at this dose regimen. Interestingly, in a subsequent study using female NMRI mice infected with *T. b. brucei* S427, **1** delivered a partial curative regimen (2/3 mice surviving to 30 d post infection; 1/3 mice with parasitaemia relapsed) when dosed at 10 mg/kg b.i.d. for 4 d. At this dose level, blood free concentration was only higher than EC₉₉ for 2 h, rapidly falling below EC₅₀ by 4 h. This indicates that whatever the mechanism of action of the compound, blood free EC₉₉ does not need to be maintained for activity as seen for *T. brucei* N-myristoyltransferase inhibitors, as observed previously.³² This could be due to rapid cidal activity, commitment to parasite death, or compound concentration selectively within the parasite.³³ Submitting compound **1** to a static-cidal assay (Figure 3) indicated the compound was rapidly cidal,³⁴ with a clear reduction of parasite counts by the first time point of the assay (24 h) at concentrations as low as 0.6 μM.

When **47** and **55** were dosed IP to female NMRI mice, a significant increase in exposure was observed compared to **1**

Table 8. Pharmacokinetic Profiles of Key Compounds^a

	1		27		35		47		55	
	IP	IP	IP	PO	IP	PO	IP	PO	IP	PO
mouse strain	HRN	NMRI	NMRI	NMRI	NMRI	NMRI	NMRI	NMRI	NMRI	NMRI
dose (mg/kg)	10	10	10	10	10	10	10	10	10	10
C _{max} (ng/mL) (μM)	2700 (8.2)	1100 (3.3)	590 (1.8)	87 (0.26)	180 (0.55)	750 (2.4)	2300 (7.4)	2900 (8.4)	1500 (4.3)	
T _{max} (h)	2	0.5	0.25	0.5	0.25	0.5	0.25	1.0	0.5	
AUC ₀₋₈ (ng min/mL) (μmol/L·h)	980,000 (50)	110,000 (5.6)	80000 (4.1)	9000 (0.46)	15,000 (0.8)	61,000 (3.3)	170,000 (9.1)	710,000 (34)	210,000 (10)	
t _{1/2} (h)	4.8	0.7	0.9	0.9	0.7	0.6	0.5	1.2	2.0	
B:B		ND	1.3		1.5	0.9	0.5	1.4		

^aB:B = brain to blood ratio (compound dosed intravenously at 0.5 or 1 mg/kg and levels measured after 5 min); ND = not determined; PO = oral; IP = intraperitoneal; AUC = area under the curve; C_{max} = the maximum concentration; T_{max} is the time at which the maximum concentration is reached; t_{1/2} is the half-life.

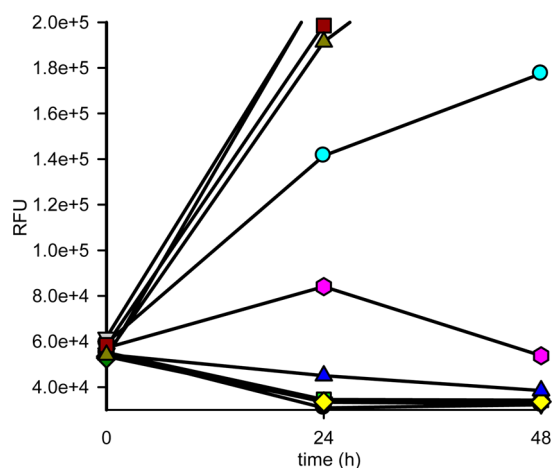


Figure 3. Static-cidal profile for *T. brucei* bloodstream form parasites were exposed to 10 concentrations of compound 1, and the effect on parasite numbers was measured at 24 and 48 h post compound exposure. A negative slope indicates cidal activity at that concentration. Concentrations are as follows (μM): (black circles) 50, (red triangles) 17, (green squares) 5.6, (yellow diamonds) 1.9, (blue triangles) 0.6, (magenta hexagons) 0.2, (cyan circles) 0.07, (violet squares) 0.01, (olive green triangles) 0. RFU = relative fluorescence units.

(1.5–6.5-fold higher AUC), consistent with the higher microsomal stability. Compound 27 had similar exposure compared to 1 (1.4-fold lower AUC), which was not surprising considering similar microsomal metabolic stability (Cl_{int} for 1 and 27 = 4.4 and 3.6 mL min⁻¹ g⁻¹, respectively). Compound 35 also had similar exposure to 1 (same AUC), yet microsomal stability was greatly improved (Cl_{int} 1.2 mL min⁻¹ g⁻¹). All compounds showed a significant loss in AUC when dosed orally.

With in vivo PoC achieved for the series in a stage 1 mouse model of HAT, it was decided to progress one of the lead molecules to a stage 2 mouse model.³⁵ All the lead compounds were brain penetrant and importantly had high brain fraction unbound (F_u), similar to plasma F_u such that significant dose adjustment above stage 1 efficacious dose should not be necessary to deliver efficacious free brain concentration. Unfortunately, however, any dose adjustment that may be required above the initial pharmacokinetic assessment would not be possible from data obtained from maximum tolerated dose (MTD) studies on 27 and 47 in female NMRI mice. Compound 47 was well tolerated at 15 mg/kg IP b.i.d. for 3 days but with clinical signs of toxicity developing at 25 mg/kg after a single dose. Compound 27 was poorly tolerated even at 15 mg/kg b.i.d. IP with clinical signs of toxicity developing during the second day of treatment.

Compound 47 was therefore chosen for the stage 2 efficacy model at a maximum dose of 12.5 mg/kg b.i.d. IP. Stage 1 efficacy data on 1 suggested time above a certain threshold was not necessary for cures. Both 47 and 55 offered the greatest improvement in C_{max} following IP dosing, but 47 was chosen for this initial study for ease of synthesis, not being a racemate and MTD already defined. For stage 2 of infection, the standard model is *T. b. brucei* GVR35 in which CNS infection is allowed to develop in female NMRI mice before treatment starts, requiring about 21 d. Mice ($n = 5$) were treated with 47 at 12.5 mg/kg IP b.i.d. for 5 d from 21 d post infection and, although the majority of mice eventually relapsed with parasitaemia (6–13 days later than vehicle dosed infected mice), one mouse was cured, defined as survival with no parasitaemia at 180 d post infection.

Screening in Receptor Panel. The compound series is very exciting as it shows partial cure in a stage 2 model of HAT. However, the observed toxicity prevents further progression of the compounds. To try and identify a possible driver for toxicity, that may then offer an opportunity to design out this unwanted effect, the key compounds were screened against a panel of receptors at the NIMH Psychoactive Drug Screening Program (PDSP).^{36,37} No significant activity against a large panel of receptors, including dopamine, serotonin, histamine, and muscarinic receptors (see [Supporting Information](#)) was observed.

SUMMARY

A series of phenoxyacyl and benzyl acyl indoline-2-carboxamides have been investigated as a new potential stage 2 therapeutic for African sleeping sickness. The series was found to be highly potent against *T. b. brucei* in culture displaying a strong antiproliferative effect while retaining excellent selectivity over the mammalian cell counter screen. The compounds showed limited possibilities for optimization; most modifications led to reduced potency or increased metabolic instability. However, a carefully designed program led to derivatives **47** and **55** with improved metabolic stability and enhanced in vivo exposure. This demonstrates that it is possible to optimize phenotypic hits in the absence of knowledge of the molecular target.³⁸

An exemplar in the series, **1** was able to cure a stage 1 model of HAT. Initially, this was carried out in HRN mice, which gave improved blood exposure. Interestingly, **1** was also curative in wild-type NMRI mice at exposures at which coverage with compound at the blood free concentration above EC₉₉ was not maintained. This indicates that whatever the mechanism of action of the compound, blood free EC₉₉ does not need to be maintained for a set duration of time, in contrast to what was required for *N*-myristoyltransferase inhibitors.³² This could be due to rapid cidalty, commitment to parasite death, or compound concentration selectively within the parasite.³³

This study demonstrates successful use of HRN mice to rapidly deliver in vivo proof of concept at a relatively early stage in the project. This gave confidence in the series and to commit additional medicinal chemistry resources to further optimization, knowing that the series was efficacious. Clearly one issue addressed in the subsequent optimization was that of microsomal stability.

Compounds in the series were brain penetrant, and partial cure in a stage 2 mouse model was achieved. Unfortunately, toxicity prevented any dose escalation to explore the possibility to deliver a fully curative stage 2 regimen. Initial attempts to identify the mode of toxicity have not been successful. Although the compounds were derived from a focused protease set, their mode of action is unknown. Elucidating the molecular target(s) may allow for a target-based drug discovery program, which may then also allow the associated toxicity with the related compounds to be dialled out.

In summary, this study has demonstrated the ability to optimize phenotypic hits to furnish compounds that are brain penetrant and trypanocidal. It has also demonstrated the utility of the HRN mice in establishing early in vivo proof of concept.

EXPERIMENTAL SECTION

Assays. Cell-Based Assays. Proliferation assays using bloodstream form *T. brucei brucei* and human MRC-5 fibroblasts were conducted using a modification of the cell viability assay as previously reported.^{27,39}

Trypanosome Growth Assay. This was conducted as previously described.²⁷ Cell culture plates were stamped with 1 μ L of an appropriate stock concentration of test compound, followed by addition of 200 μ L of trypanosome culture (HMI9-T, 10% FCS) to each well at a density of 2000 cells per well (except column 12 receiving media only). Primary screening was carried out at 30 μ M; 93 compounds showed a greater than 50% inhibition of parasite growth. Potency was carried out using 10-point dose–response curves.

MRC-5 Growth Assay. This was conducted as previously described.²⁷ MRC-5 cells (2000 cells per well) were seeded in 200 μ L of DMEM, 10% FCS, and allowed to adhere overnight. One microliter of test compound was added to each well on the day of assay initiation.

Trypanosome and MRC-5 plates were incubated at 37 °C in an atmosphere of 5% CO₂ for 69 h prior to the addition of 20 μ L of rezasurin (final concentration 50 μ M). After a further 4 h, fluorescence was measured (excitation 528 nm; emission 590 nm) using a BioTek flx800 plate reader. For cell assays, ten-point screening was conducted between 15 μ M and 0.5 nM or between 50 μ M and 2 nM, depending on stock concentrations. The final DMSO level was 0.5% in all cases.

Static-Cidal Assay. The static-cidal assay was conducted as previously described.³⁴ In short, bloodstream-form *T. brucei* cells were plated into 384-well assay plates (4 \times 10⁵ cell mL⁻¹, 50 μ L/well) and incubated for 0, 20 or 44 h at 37 °C, 5% CO₂. At each time-point, plates were developed with resazurin as described above.

Physicochemical Properties and in Vitro DMPK Parameters.

The software package StarDrop by Optibrium was used to calculate physicochemical parameters including log *P*, molecular weight, and polar surface area (PSA). The aqueous kinetic solubility of the compounds was measured using laser nephelometry as previously described.⁴⁰ The plasma protein binding of the compounds was determined by the equilibrium dialysis method.¹²

Brain Tissue Binding. The methodology employed was a modification of that reported previously (Summerfield et al., 2007).⁴¹ In brief, a 96-well equilibrium dialysis apparatus was used to determine the free fraction in the brain for the test compound (HT Dialysis LLC, Gales Ferry, CT). Membranes (12–14 kDa A cutoff) were conditioned in deionized water for 60 min, followed by conditioning in 80:20 deionized water:ethanol for 20 min and then rinsed in artificial cerebrospinal fluid (CSF) before use. Mouse brain was removed from the freezer and allowed to thaw on the day of experiment. Thawed brain tissue was homogenized with artificial CSF to a final composition of 1:2 brain:artificial CSF using a Covaris S2 (KBiosciences, Hoddesdon, UK). Diluted brain homogenate was spiked with the test compound (10 μ g/g), and 150 μ L aliquots (*n* = 6 replicate determinations) loaded into the 96-well equilibrium dialysis plate. Dialysis vs artificial CSF (150 μ L) was carried out for 5 h in a temperature controlled incubator at ca. 37 °C (Stuart scientific Ltd., UK) using an orbital microplate shaker at 125 rpm (Stuart scientific Ltd., UK). At the end of the incubation period, aliquots of brain homogenate or artificial CSF were transferred to micronic tubes (Micronic BV, The Netherlands) and the composition in each tube balanced with control fluid such that the volume of artificial CSF to brain homogenate is the same. Sample extraction was performed by the addition of 400 μ L of acetonitrile containing an appropriate internal standard. Samples were allowed to mix for 1 min and then centrifuged at 1825g in 96-well blocks for 10 min (Allegra X12-R, Beckman Coulter, USA). All samples were analyzed by means of UPLC/MS/MS on a Quattro Premier XE mass spectrometer (Waters Corporation, USA). The unbound fraction was determined as the ratio of the peak area in artificial CSF to that in brain, with correction for dilution factor according to eq 1.⁴²

$$\text{undiluted } F_u = \frac{1/D}{((1/F_{u,\text{apparent}}) - 1) + 1/D} \quad (1)$$

where *D* = dilution factor in brain homogenate and *F*_{u,apparent} is the measured free fraction of diluted brain homogenate.

Intrinsic Clearance (Cl_{int}) Determination. Each test compound (0.5 μ M) was incubated with pooled female CDI mouse liver microsomes, pooled male Sprague–Dawley rat microsomes, or pooled mixed gender human liver microsomes (Tebu-Bio, UK; 0.5 mg/mL 50

mM potassium phosphate buffer, pH 7.4) and the reaction started with addition of excess NADPH (8 mg/mL, 50 mM potassium phosphate buffer, pH 7.4). Immediately, at time zero, then at 3, 6, 9, 15, and 30 min, an aliquot (50 μ L) of the incubation mixture was removed and mixed with acetonitrile (100 μ L) to stop the reaction. Internal standard was added to all samples, and the samples were centrifuged at 1825g for 10 min to sediment precipitated protein. The plates were then sealed prior to UPLC/MS/MS analysis using a Quattro Premier XE (Waters Corporation, USA).

XLfit (IDBS, UK) was used to calculate the exponential decay and consequently the rate constant (k) from the ratio of peak area of test compound to internal standard at each time point. The rate of intrinsic clearance (Cl_{int}) of each compound was then calculated using the following eq 2:

$$Cl_{int} (\text{mL min}^{-1} \text{ g}^{-1} \text{ liver}) = k \times V \times \text{microsomal protein yield} \quad (2)$$

where V (mL/mg protein) is the incubation volume/mg protein added and microsomal protein yield is taken as 52.5 mg protein/g liver.⁴³ Verapamil was used as a positive control to confirm acceptable assay performance.

In Vivo Mouse Pharmacokinetics and Brain Penetration. *Mouse Pharmacokinetics.* Each compound was dosed as a bolus solution intraperitoneally at 10 mg free base/kg (dose volume, 10 mL/kg; dose vehicles used, 10% DMSO; 40% PEG400; 50% Milli-Q water or 5% DMSO; 40% PEG400; 55% saline) to female HRN (1 only) or NMRI mice ($n = 3$) or dosed orally by gavage as a solution at 10 mg free base/kg (dose volume, 10 mL/kg; dose vehicle, 10% DMSO; 40% PEG400; 50% Milli-Q water) to female NMRI mice ($n = 3$). Female NMRI mice were chosen, as these represent the sex and strain used for the stage 1 and stage 2 HAT efficacy models. Blood samples were taken from each mouse at 5 (IP only), 15, and 30 min, 1, 2, 4, 6, and 8 h post dose, mixed with two volumes of distilled water, and stored frozen until UPLC/MS/MS analysis. Pharmacokinetic parameters were derived from noncompartmental analysis of the blood concentration time curve using PK solutions software v 2.0 (Summit Research Services, USA).

Mouse Brain Penetration. Each compound was dosed as a bolus solution intravenously at 0.5 or 1 mg free base/kg (dose volume, 5 mL/kg; dose vehicle, 10% DMSO; 40% PEG400; 50% Milli-Q water) to female NMRI mice ($n = 6$). At 5 and 30 min following intravenous bolus injection of test compound, mice ($n = 3$ /time point) were placed under terminal anesthesia with isoflurane. A blood sample was taken by cardiac puncture and mixed with two volumes of distilled water, the mice decapitated, and the brain removed. Diluted blood and brains were stored frozen until preparation and analysis by UPLC/MS/MS. For each mouse at each time point, the concentration in brain (ng/g) was divided by the concentration in blood (ng/mL) to give a brain: blood ratio. The mean value obtained was quoted.

Mouse Stage-1 and Stage-2 Efficacy Mouse Models. These were carried out as previously described^{27,32} at the dose level presented and using the same dose formulation as the pharmacokinetic studies. HRN mice were used under the same infection and monitoring protocol as described for female NMRI mice.

Animal Ethics. All regulated procedures on living animals were carried out under the authority of a project license issued by the Home Office under the Animals (Scientific Procedures) Act 1986, as amended in 2012 (and in compliance with EU Directive EU/2010/63). License applications were approved by the University's Ethical Review Committee (ERC) before submission to the Home Office. The ERC has a general remit to develop and oversee policy on all aspects of the use of animals on University premises and is a subcommittee of the University Court, its highest governing body.

Chemistry/Compound Characterization. *General Methods.* Chemicals and solvents were purchased from Aldrich Chemical Co., Alfa Aesar, Fluorochem, Apollo, and Fisher Chemicals and were used as received unless otherwise stated. Air- and moisture-sensitive reactions were carried out under an inert atmosphere of argon in oven-dried glassware. Analytical thin-layer chromatography (TLC) was performed on precoated TLC plates (layer 0.20 mm silica gel 60 with fluorescent indicator UV254, from Merck). Developed plates were air-dried and

analyzed under a UV lamp (UV 254/365 nm) and/or KMnO_4 was used for visualization. Flash column chromatography was performed on an automated purification system (Teledyne ISCO Combiflash Companion or Combiflash Retrieve) using Grace Resolve preppacked silica gel cartridges (230–400 mesh, 40–63 μ m, varying sizes depending on reaction scale). ^1H and ^{13}C NMR spectra were recorded on a Bruker Advance II 500 spectrometer operating at 500.1 and 125.8 MHz (unless otherwise stated) using CDCl_3 or $\text{DMSO}-d_6$ solutions. Chemical shifts (δ) are expressed in ppm recorded using the residual solvent as the internal reference in all cases. Signal splitting patterns are described as singlet (s), doublet (d), triplet (t), multiplet (m), broadened (b), or a combination thereof. Coupling constants (J) are quoted to the nearest 0.1 Hz (Hz). LC-MS analyses were performed with either an Agilent HPLC 1100 series connected to a Bruker Daltonics MicroTOF or an Agilent Technologies 1200 series HPLC connected to an Agilent Technologies 6130 quadrupole spectrometer, where both instruments were connected to an agilent diode array detector. LC-MS chromatographic separations were conducted with a Water Xbridge C18 column, 50 mm \times 2.1 mm, 3.5 μ m particle size, using either methanol, methanol/water (95:5), or water/acetonitrile (1:1) + 0.1% formic acid as the mobile phase; linear gradient from 80:20 to 5:95 over 3.5 min and then held for 1.5 min; flow rate of 0.5 mL min^{-1} . All synthesized compounds were determined to be of >95% purity by the LC-MS method (TIC and UV) as determined using this analytical LC-MS system. High resolution electrospray measurements were performed on a Bruker MicroTof mass spectrometer. Microwave-assisted chemistry was performed using a Biotage Initiator microwave synthesizer.

General Procedure A: Synthesis of Diamides from Indoline-2-carboxylic Acid (Scheme 1). To a solution of $\text{R}^1\text{CO}_2\text{H}$ (1 mol equiv) in DCM (anhydrous, 5 mL mmol^{-1}) at room temperature, *O*-(benzotriazol-1-yl)-*N,N,N',N'*-tetramethyluronium tetrafluoroborate (TBTU) (1 mol equiv) was added and the reaction mixture stirred for 30 min, indoline-2-carboxylic acid (1 mol equiv) was then added and the reaction mixture stirred for 2 h. The progress of the reaction was monitored by LCMS; after successful coupling of the first amide, a further 1 equiv of TBTU was added to the reaction mixture and the mixture stirred for 30 min, methylamine (2 M in MeOH or 2 M in THF, 5 mol equiv) was added, and the reaction mixture stirred for a further 1 h or until complete consumption of the starting material was observed. The reaction was quenched with H_2O , passed through a hydrophobic frit, and the organic layer concentrated in vacuo. Column chromatography eluting with ether afforded the desired diamides.

(R)-1-(2-(4-Chlorophenoxy)acetyl)-*N*-methylinoline-2-carboxamide (27). Prepared using general procedure A, colorless solid, 207 mg, 67%. δ_{H} (500 MHz, CDCl_3) 8.21 (bs, 1H, NH), 7.30–7.26 (m, 5H, ArH), 7.15 (t, $J = 7.5$ Hz, 1H, ArH), 6.91 (dd, $J = 6.9$ and 2.2 Hz, 2H, ArH), 5.79 and 5.06 (2 \times bs, rotomer, 1H, CH_2), 5.28 and 4.75 (2 \times bs, rotomer, 2H, CH_2), 3.68 (bs, 1H, CH_2), 3.30 (bs, 1H, CH_2), 2.76 (bd, rotomer, 3H, CH_3). δ_{C} (125 MHz, $\text{DMSO}-d_6$) 171.0, 165.9 (C=O), 156.9, 142.8, 129.6, 129.0, 127.1, 124.6, 124.5, 123.7, 116.2 (ArC), 66.0, 59.6, 34.5, 25.9. LCMS (ES+): m/z (%) 345 [$\text{M} + \text{H}$]⁺. t_{R} : 4.17 (20–95% MeCN, acidic). HRMS (ES+) calcd for [$\text{C}_{18}\text{H}_{18}\text{ClN}_2\text{O}_3 + \text{H}$], 345.1000; found, 345.0988.

(R)-1-(2-(4-Fluorophenyl)acetyl)-*N*-methylinoline-2-carboxamide (47). Prepared using general procedure A, colorless solid, 339 mg, 54%. δ_{H} (500 MHz, $\text{DMSO}-d_6$) 8.28 (d, $J = 4.4$ Hz, 1H, NH), 8.05 (d, $J = 8.1$ Hz, 1H, ArH), 7.28–7.26 (m, 2H, ArH), 7.21 (d, $J = 7.3$ Hz, 1H, ArH), 7.17–7.13 (m, 2H, ArH), 7.01 (t, $J = 7.3$ Hz, 1H, ArH), 5.11 (d, $J = 8.7$ Hz, 1H, CH), 3.78 (d, $J = 16.0$ Hz, 1H, CH_2), 3.59 (dd, $J = 16.5$ and 11.3 Hz, 1H, CH_2), 3.47 (d, $J = 16.0$ Hz, 1H, CH_2), 3.06 (d, $J = 16.5$, 1H, CH_2), 2.65 (d, $J = 4.4$ Hz, 3H, CH_3). δ_{C} (125 MHz, $\text{DMSO}-d_6$) = 171.4 (C=O), 169.3 (C=O), 131.6, 131.85, 131.2, 130.0, 127.0, 124.4, 123.4, 116.3, 114.9, 114.7 (ArC), 60.9, 34.1, 25.8. LCMS (ES+): m/z (%) 313 [$\text{M} + \text{H}$]⁺. t_{R} : 3.90 (20–95% MeCN, acidic). HRMS (ES+) calcd for [$\text{C}_{18}\text{H}_{18}\text{FN}_2\text{O}_2 + \text{H}$], 313.1347; found, 313.1335.

■ ASSOCIATED CONTENT

■ Supporting Information

The Supporting Information is available free of charge on the ACS Publications website at DOI: 10.1021/acs.jmedchem.5b00596.

Synthetic details for 26, 28–55, 13, 57–68; details of receptors screened at the NIMH Psychoactive Drug Screening Program (PDF)
Molecular formula strings (CSV)

■ AUTHOR INFORMATION

Corresponding Author

*Phone: +44 1382 386 240. E-mail: i.h.gilbert@dundee.ac.uk.

Notes

The authors declare no competing financial interest.

■ ACKNOWLEDGMENTS

Funding for this work was provided by the Wellcome Trust (grant ref. WT077705 and Strategic Award WT083481). We thank Dr. Stephen Thompson and Margaret Huggett for chemical synthesis around the indoline-2-carboxamide not detailed here, Gina McKay for performing HRMS analyses, and Daniel James for data management. Receptor binding profiles were generously provided by the National Institute of Mental Health's Psychoactive Drug Screening Program, contract no. HHSN-271-2008-00025-C (NIMH PDSP). The NIMH PDSP is directed by Bryan L. Roth MD, Ph.D., at the University of North Carolina at Chapel Hill and Project Officer Jamie Driscoll at NIMH, Bethesda MD, USA.

■ ABBREVIATIONS USED

HAT, human African trypanosomiasis; *T.b.*, *Trypanosoma brucei*; HTS, high throughput screening; F_w , fraction unbound; PPB, plasma protein binding; SAR, structure–activity relationship; DMPK, drug metabolism and pharmacokinetics; TBTU, O-(benzotriazol-1-yl)-N,N,N',N'-tetramethyluronium tetrafluoroborate; CLEA, *Candida antartica* CAL-A; Cl_{int} , intrinsic clearance; B:B, blood to brain ratio; CNS, central nervous system

■ REFERENCES

- (1) Stuart, K. D.; Brun, R.; Croft, S. L.; Fairlamb, A.; Gurtler, R. E.; McKerrow, J. H.; Reed, S.; Tarleton, R. Kinetoplastids: related protozoan pathogens, different diseases. *J. Clin. Invest.* **2008**, *118*, 1301–1310.
- (2) Brun, R.; Don, R.; Jacobs, R. T.; Wang, M. Z.; Barrett, M. P. Development of novel drugs for human African trypanosomiasis. *Future Microbiol.* **2011**, *6*, 677–691.
- (3) Barrett, M. P.; Croft, S. L. Management of trypanosomiasis and leishmaniasis. *Br. Med. Bull.* **2012**, *104*, 175–196.
- (4) Field, M. C. Drug Screening by crossing membranes: a novel approach to identification of trypanocides. *Biochem. J.* **2009**, *419*, e1–e3.
- (5) Bouteille, B.; Oukem, O.; Bisser, S.; Dumas, M. Treatment perspectives for human African trypanosomiasis. *Fundam. Clin. Pharmacol.* **2003**, *17*, 171–181.
- (6) Barrett, M. P.; Boykin, D. W.; Brun, R.; Tidwell, R. R. Human African trypanosomiasis: pharmacological re-engagement with a neglected disease. *Br. J. Pharmacol.* **2007**, *152*, 1155–1171.
- (7) Castillo, E.; Dea-Ayuela, M. A.; Fernandes-Bolas, F.; Rangel, M.; Gonzalez-Rosende, M. E. The Kinetoplastid chemotherapy revisited: current drugs, recent advances and future perspectives. *Curr. Med. Chem.* **2010**, *17*, 4027–4051.
- (8) Priotto, G.; Kasparian, S.; Mutombo, W.; Ngouama, D.; Ghorashian, S.; Arnold, U.; Ghabri, S.; Baudin, E.; Buard, V.; Kazadi-

Kyanza, S.; Ilunga, M.; Mutangala, W.; Pohlig, G.; Schmid, C.; Karunakara, U.; Torreale, E.; Kande, V. Nifurtimox-eflornithine combination therapy for second-stage African *Trypanosoma brucei gambiense* trypanosomiasis: a multicentre, randomised, phase III, non-inferiority trial. *Lancet* **2009**, *374*, 56–64.

(9) Yun, O.; Priotto, G.; Tong, J.; Flevaud, L.; Chappuis, F. NECT is next: implementing the new drug combination therapy for *Trypanosoma brucei gambiense* sleeping sickness. *PLoS Neglected Trop. Dis.* **2010**, *4*, e720.

(10) Sokolova, A. Y.; Wyllie, S.; Patterson, S.; Oza, S. L.; Read, K. D.; Fairlamb, A. H. Cross-resistance to nitro drugs and implications for treatment of human African trypanosomiasis. *Antimicrob. Agents Chemother.* **2010**, *54*, 2893–2900.

(11) Chatelain, E.; Iset, J.-R. Drug discovery and development for neglected diseases: the DNDi model. *Drug Des., Dev. Ther.* **2011**, *5*, 175–181.

(12) Jones, D. C.; Hallyburton, I.; Stojanovski, L.; Read, K. D.; Frearson, J. A.; Fairlamb, A. H. Identification of a k-opioid agonist as a potent and selective lead for drug development against human African trypanosomiasis. *Biochem. Pharmacol.* **2010**, *80*, 1478–1486.

(13) Smith, V. C.; Cleghorn, L. A.; Woodland, A.; Spinks, D.; Hallyburton, I.; Collie, I. T.; Mok, N. Y.; Norval, S.; Brenk, R.; Fairlamb, A. H.; Frearson, J. A.; Read, K. D.; Gilbert, I. H.; Wyatt, P. G. Optimisation of the anti-*Trypanosoma brucei* activity of the opioid agonist U50488. *ChemMedChem* **2011**, *6*, 1832–1840.

(14) Gilbert, I. H. Drug discovery for neglected diseases: Molecular target-based and phenotypic approaches. *J. Med. Chem.* **2013**, *56*, 7719–7726.

(15) Brenk, R.; Schipani, A.; James, D.; Krasowski, A.; Gilbert, I. H.; Frearson, J.; Wyatt, P. G. Lessons learnt from assembling screening libraries for drug discovery for neglected diseases. *ChemMedChem* **2008**, *3*, 435–444.

(16) Kelder, J.; Grootenhuis, P. D. J.; Bayada, D. M.; Delbressine, L. P. C.; Ploemen, J. P. Polar molecular surface as a dominating determinant for oral absorption and brain penetration of drugs. *Pharm. Res.* **1999**, *16*, 1514–1519.

(17) Wager, T. T.; Chandrasekaran, R. Y.; Hou, X.; Troutman, M. D.; Verhoest, P. R.; Villalobos, A.; Will, Y. Defining desirable Central Nervous System drug space through the alignment of molecular properties, in vitro ADME, and safety attributes. *ACS Chem. Neurosci.* **2010**, *1*, 420–434.

(18) Wager, T. T.; Hou, X.; Verhoest, P. R.; Villalobos, A. Moving beyond rules: The development of a Central Nervous System Multiparameter Optimization (CNS MPO) approach to enable alignment of drug-like properties. *ACS Chem. Neurosci.* **2010**, *1*, 435–449.

(19) Gilbert, I. H. Target-based drug discovery for human African trypanosomiasis: selection of molecular target and chemical matter. *Parasitology* **2014**, *141*, 28–36.

(20) Roy, P.; Boisvert, M.; Leblanc, Y. Preparation of substituted 5-azaindoles: Mety 4-chloro-1H-pyrrolo[3,2-C]pyridine-2-carboxylate. *Org. Synth.* **2007**, *84*, 262–271.

(21) Stokes, B.; Dong, H.; Leslie, B.; Pumphrey, A.; Driver, T. Intramolecular C-H aminations reactions: Exploitation of the Rh-2(II)-Catalysed decomposition of azidoacrylates. *J. Am. Chem. Soc.* **2007**, *129*, 7500–7501.

(22) Youn, I.; Pak, C. Reduction of indole-2-carboxylate and 2-carboxamide with magnesium in methanol. *Bull. Korean Chem. Soc.* **1987**, *8*, 434–435.

(23) Ooi, T.; Uematsu, Y.; Maruoka, K. Highly enantioselective alkylation of glycine methyl and ethyl ester derivatives under phase-transfer conditions: it synthetic advantage. *Tetrahedron Lett.* **2004**, *45*, 1675–1678.

(24) Kitamura, M.; Arimura, Y.; Shirakawa, S.; Maruoka, K. Combinatorial approach for the design of new, simplified chiral phase-transfer catalysts with high catalytic performance for practical asymmetric synthesis of alpha-alkyl-alpha-amino acids. *Tetrahedron Lett.* **2008**, *49*, 2026–2030.

- (25) Ooi, T.; Kameda, M.; Maruoka, K. Design of N-spiro C-2-symmetric chiral quaternary ammonium bromides as novel chiral phase-transfer catalysts: Synthesis and application to practical asymmetric synthesis of alpha-amino acids. *J. Am. Chem. Soc.* **2003**, *125*, 5139–5151.
- (26) Alatorre-Santamaria, S.; Rodriguez-Mata, M.; Gotor-Fernandez, V.; de Mattos, M. C.; Sayago, F. J.; Jimenez, A. L.; Catiuela, C.; Gotor, V. Efficient access to enantiomerically pure cyclic alpha-amino esters through a lipase-catalyzed kinetic resolution. *Tetrahedron: Asymmetry* **2008**, *19*, 1714–1719.
- (27) Brand, S.; Cleghorn, L. A.; McElroy, S. P.; Robinson, D. A.; Smith, V. C.; Hallyburton, I.; Harrison, J. R.; Norcross, N. R.; Spinks, D.; Bayliss, T.; Norval, S.; Stojanovski, L.; Torrie, L. S.; Frearson, J. A.; Brenk, R.; Fairlamb, A. H.; Ferguson, M. A.; Read, K. D.; Wyatt, P. G.; Gilbert, I. H. Discovery of a novel class of orally active trypanocidal N-myristoyltransferase inhibitors. *J. Med. Chem.* **2012**, *55*, 140–152.
- (28) Meanwell, N. A. Synopsis of some recent tactical application of bioisosteres in drug design. *J. Med. Chem.* **2011**, *54*, 2529–2591.
- (29) Böhm, H.; Banner, D.; Bendels, S.; Kansy, M.; Kuhn, B.; Müller, K.; Obst-Sander, U.; Stahl, M. Fluorine in medicinal chemistry. *ChemBioChem* **2004**, *5*, 637–643.
- (30) Wagaw, S.; Yang, B.; Buchwald, S. A palladium-catalyzed strategy for the preparation of indoles: a novel entry into the Fischer indole synthesis. *J. Am. Chem. Soc.* **1998**, *120*, 6621–6622.
- (31) Pass, G. J.; Carrie, D.; Boylan, N.; Lorimore, S.; Wright, E.; Houston, B.; Henderson, C. J.; Wolf, C. R. Role of hepatic cytochrome P450s in the pharmacokinetics and toxicity of cyclophosphamide: Studies with the hepatic cytochrome P450 reductase null mouse. *Cancer Res.* **2005**, *65*, 4211–4217.
- (32) Frearson, J. A.; Brand, S.; McElroy, S. P.; Cleghorn, L. A.; Smid, O.; Stojanovski, L.; Price, H. P.; Guthrie, M. L.; Torrie, L. S.; Robinson, D. A.; Hallyburton, I.; Mpamhanga, C. P.; Brannigan, J. A.; Wilkinson, A. J.; Hodgkinson, M.; Hui, R.; Qiu, W.; Raimi, O. G.; van Aalten, D. M.; Brenk, R.; Gilbert, I. H.; Read, K. D.; Fairlamb, A. H.; Ferguson, M. A.; Smith, D. F.; Wyatt, P. G. N-myristoyltransferase inhibitors as new leads to treat sleeping sickness. *Nature* **2010**, *464*, 728–32.
- (33) Barrett, M. P.; Gilbert, I. H. Targeting of toxic compounds to the trypanosomes. *Adv. Parasitol.* **2006**, *63*, 126–183.
- (34) De Rycker, M.; O'Neill, S.; Joshi, D.; Campbell, L.; Gray, D. W.; Fairlamb, A. H. A static-cidal assay for *Trypanosoma brucei* to aid hit prioritisation for progression into drug discovery programmes. *PLoS Neglected Trop. Dis.* **2012**, *6*, e1932.
- (35) Jennings, F. W.; Urquhart, G. M.; Murray, P. K.; Miller, B. M. Treatment with suranim and 2-substituted 5-nitroimidazoles of chronic murine *Trypanosoma brucei* infections with central nervous system involvement. *Trans. R. Soc. Trop. Med. Hyg.* **1983**, *77*, 693–698.
- (36) Jensen, N. H.; Roth, B. L. Massively parallel screening of the receptorome. *Comb. Chem. High Throughput Screening* **2008**, *11*, 420–426.
- (37) Besnard, J.; Ruda, G. F.; Setola, V.; Abecassis, K.; Rodriguez, R. M.; Huang, X. P.; Norval, S.; Sassano, M. F.; Shin, A. I.; Webster, L. A.; Simeons, F. R.; Stojanovski, L.; Prat, A.; Seidah, N. G.; Constam, D. B.; Bickerton, G. R.; Read, K. D.; Wetsel, W. C.; Gilbert, I. H.; Roth, B. L.; Hopkins, A. L. Automated design of ligands to polypharmacological profiles. *Nature* **2012**, *492*, 215–220.
- (38) Gilbert, I. H.; Leroy, D.; Frearson, J. A. Finding new hits in neglected disease projects: Target or phenotypic based screening? *Curr. Top. Med. Chem.* **2011**, *11*, 1284–1291.
- (39) Raz, B.; Iten, M.; Grether-Bühler, Y.; Kaminsky, R.; Brun, R. The Alamar Blue assay to determine drug sensitivity of African trypanosomes (*T. b. rhodesiense* and *T. b. gambiense*) in vitro. *Acta Trop.* **1997**, *68*, 139–147.
- (40) Patterson, S.; Wyllie, S.; Stojanovski, L.; Perry, M. R.; Simeons, F. R.; Norval, S.; Osuna-Cabello, M.; De Rycker, M.; Read, K. D.; Fairlamb, A. H. The R enantiomer of the antitubercular drug PA-824 as a potential oral treatment for visceral Leishmaniasis. *Antimicrob. Agents Chemother.* **2013**, *57*, 4699–4706.
- (41) Summerfield, S. G.; Read, K.; Begley, D. J.; Obradovic, T.; Hidalgo, I. J.; Coggon, S.; Lewis, A. V.; Porter, R. A.; Jeffrey, P. Central nervous system drug disposition: the relationship between in situ brain permeability and brain free fraction. *J. Pharmacol. Exp. Ther.* **2007**, *322*, 205–213.
- (42) Kalvass, J. C.; Maurer, T. S. Influence of nonspecific brain and plasma binding on CNS exposure: implications for rational drug discovery. *Biopharm. Drug Dispos.* **2002**, *23*, 327–338.
- (43) Iwatsubo, T.; Suzuki, H.; Shimada, N.; Chiba, K.; Ishizaki, T.; Green, C. E.; Tyson, C. A.; Yokoi, T.; Kamataki, T.; Sugiyama, Y. Prediction of in vivo hepatic metabolic clearance of YM796 from in vitro data by use of human liver microsomes and recombinant P-450 isozymes. *J. Pharmacol. Exp. Ther.* **1997**, *282*, 909–919.